

See discussions, stats, and author profiles for this publication at: <https://www.researchgate.net/publication/228636509>

CO Oxidation on Pt-Group Metals from Ultrahigh Vacuum to Near Atmospheric Pressures. 2. Palladium and Platinum

ARTICLE *in* THE JOURNAL OF PHYSICAL CHEMISTRY C · JANUARY 2009

Impact Factor: 4.77 · DOI: 10.1021/jp8077985

CITATIONS

91

READS

40

4 AUTHORS, INCLUDING:



Yun Cai

General Motors Company

29 PUBLICATIONS 1,243 CITATIONS

SEE PROFILE

CO Oxidation on Pt-Group Metals from Ultrahigh Vacuum to Near Atmospheric Pressures. 2. Palladium and Platinum

F. Gao, Y. Wang, Y. Cai, and D. W. Goodman*

Department of Chemistry, Texas A&M University, P.O. Box 30012, College Station, Texas 77842-3012

Received: September 2, 2008; Revised Manuscript Received: November 3, 2008

CO oxidation on Pd(100), -(111), -(110), and Pt(110) single crystals was studied at steady-state conditions at low ($\leq 2 \times 10^{-3}$ Torr) and high (2–88 Torr) pressures at various reactant compositions. At low pressures the reaction fell into two regimes, one with a CO-dominant surface where the CO₂ formation rate is low, and a second with an O-dominant surface where the reaction rate is high. Within this second regime, the reaction is collision-limited with no oxygen inhibition. Under high-pressure reaction conditions, three reaction regimes are evident: (i) a CO-inhibited metallic regime displaying a low CO₂ formation rate; (ii) an oxygen-rich metallic regime with a high CO₂ formation rate; and (iii) a high-temperature regime where the CO₂ formation rate is either mass transfer limited on a metallic surface or limited by the reduced reactivity of the oxidized surface. The superior activity of Pt group metal oxides compared to the reduced metal, as proposed recently, was not observed in this study.

1. Introduction

We have shown previously¹ that for Rh(111), oxygen inhibition of the CO oxidation reaction occurs at low pressures ($\leq 2 \times 10^{-3}$ Torr) even at oxygen coverages of ~ 0.5 monolayers (ML). At high pressures (2–88 Torr), even though the surface is still quite active as the oxygen coverage approaches ~ 1 ML, the surface deactivates substantially upon further oxidation.¹ These results are consistent with earlier studies^{2,3} but completely contradict the recent conclusions drawn by Frenken et al.^{4–6} regarding the “superior reactivity” of oxide phases toward CO oxidation. In the present work, we present results on CO oxidation over Pd and Pt single crystal surfaces, including the Pd(100) and Pt(110) surfaces used by Frenken et al. in their studies, confirming that their conclusions regarding the “superior reactivity” of an oxide phase are incorrect. This erroneous conclusion was arrived at because the authors were not aware of a highly active state lying between the low-temperature CO-poisoned state and the mass transfer limited high-temperature state. This catalytic state, referred to previously as a “hyperactive” state,⁷ is a chemisorbed oxygen-dominant state.

2. Experimental Section

The apparatus and experimental procedure for this study are described in detail in the previous paper.¹ Except for slight differences in sample cleaning, the experimental procedures are identical.

3. Results

3.1. Steady-State Reactions at Low Pressures. Low-pressure CO oxidation on Pd and Pt surfaces has been studied extensively, and the reaction mechanism and kinetics are very well understood.⁸ Nevertheless, low-pressure reaction kinetics have been carried out in the present study in order to test for continuity between the low- and high-pressure regimes. Figure 1 displays an example of a rate measurement on Pd(100) using

an O₂/CO mixture (1/1) at a CO pressure of 1×10^{-6} Torr. Figure 1a is a plot of the CO₂ formation rate (turnover frequency, TOF, CO₂ molecule site⁻¹ s⁻¹) at various reaction temperatures. The details for calculating the reaction rate are described in the previous paper.¹ Figure 1b shows the corresponding polarization modulation infrared reflection absorption spectroscopy (PM-IRAS) spectra at various temperatures. Under such reaction conditions only bridging CO features, which red shift with increasing temperature, are detected. There are several salient points to mention regarding these data. First, the reaction can be divided into two regimes: a low-rate regime on a CO-dominant surface and a high-rate regime where the surface CO coverage is below the detection limit of IRAS, i.e., below ~ 0.01 monolayer. Second, it is seen that at any given reaction temperature, the reaction rate remains extremely constant with time. Note that this is rather distinct from Rh(111) for which the rate of reaction diminishes with time at relatively high temperatures.¹ This suggests that the oxygen inhibition present with Rh(111) is not found with Pd. Finally, the CO PM-IRAS spectra display lineshapes and vibrational frequencies similar to CO on clean Pd(100) at ≤ 475 K at 1×10^{-6} Torr CO.⁹ This suggests that under steady-state conditions, the oxygen coverage never becomes high enough to limit the adsorption of sufficient quantities of CO. Similar steady-state experiments were also performed with reactants of various O₂/CO ratios (from 1/2 to 10/1) and various CO pressures (from 1×10^{-8} to 1×10^{-3} Torr) over Pd(100), (111) and (110) surfaces.

Figure 2 presents the relationship between the surface CO coverage and the CO reaction probability over Pd(100) with stoichiometric mixtures of CO pressures ranging from 1×10^{-8} to 1×10^{-3} Torr. In this case, the upper panel displays the integrated CO (bridging only) peak areas and the bottom panel presents the CO reaction probability, both as a function of reaction temperature. At all pressures, the CO₂ formation commences only when the CO peak area begins to decrease, i.e., the CO coverage becomes less than ~ 0.6 ML.⁹ It is also found, without exception, that at all pressures the CO₂ formation maximizes at the point where the CO PM-IRAS signal falls to zero. Note that for other O₂/CO ratios, similar results are found.

* Corresponding author: tel, +1 979 845 0214; fax, +1 979 845 6822; e-mail, goodman@mail.chem.tamu.edu (D.W. Goodman).

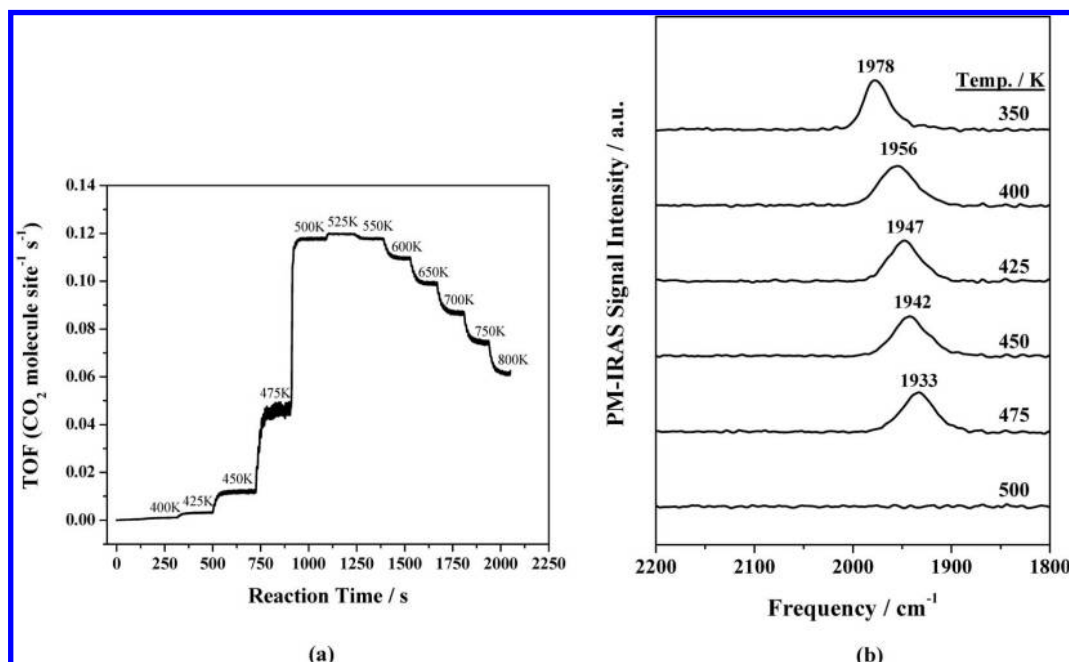


Figure 1. (a) Steady-state CO_2 formation rate (TOF) of O_2/CO (1/1) mixture over Pd(100) at CO pressure of 1×10^{-6} Torr as a function of temperature. (b) PM-IRAS spectra of O_2/CO (1/1) mixture over Pd(100) at CO pressure of 1×10^{-6} Torr as a function of temperature. Sample temperatures are marked adjacent to each spectrum. Note that no surface CO species is detectable at 500 K and above.

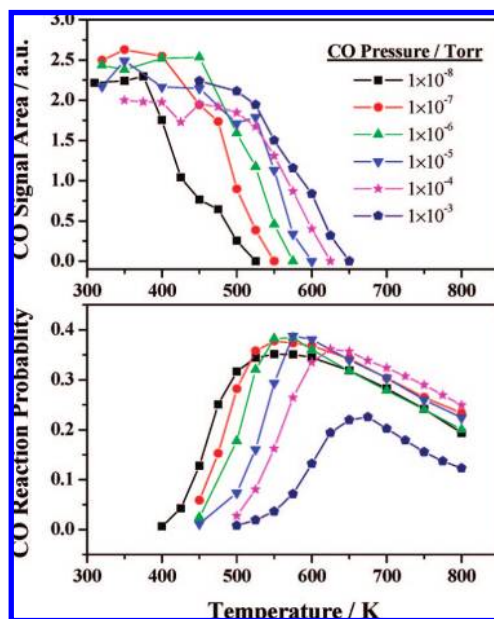


Figure 2. CO PM-IRAS signal area (upper panel) and reaction probability (bottom panel) as a function of reaction temperature for O_2/CO (1/2) mixtures at various pressures. Data obtained at different CO pressures are presented with different symbols.

Moreover, it is shown in the bottom panel of Figure 2 that the maximum CO reaction probability remains very constant at 35–40% for CO pressures between 1×10^{-8} to 1×10^{-4} Torr. However, the reaction probability drops to $\sim 20\%$ upon increasing the CO pressure to 1×10^{-3} Torr. Clearly the reaction is collision limited at CO pressures of 1×10^{-4} Torr and below while the effect of mass transfer becomes important at higher pressures. As will be shown below, the limitation of mass transfer becomes more pronounced at higher pressures.

Figure 3 displays a typical steady-state reaction on Pt(110). For this set of data, the reactants consist of an O_2/CO mixture (1/1) at a CO pressure of 1×10^{-3} Torr. In Figure 3a, which

shows PM-IRAS spectra acquired at various reaction temperatures, only atop CO features are detected. Figure 3b plots the CO signal area (upper panel) and CO_2 formation rate (bottom panel) versus the reaction temperature. As seen previously for Pd surfaces, as the CO_2 formation rate reaches a maximum, the adsorbed CO signal approaches zero. Finally, in order to achieve a CO_2 formation rate for reactant conditions similar to those found for Pd, the reaction temperature required for Pt(110) is some 50–100 K higher (data not shown). Clearly CO inhibition is a key factor even to higher temperatures for Pt. This does not mean that CO binds more strongly to Pt⁸ but rather suggests that higher reaction temperatures are required to activate O_2 dissociation on Pt. It is noteworthy that oxygen inhibition was not found under any reaction conditions during low-pressure steady-state studies on Pt or Pd surfaces.

3.2. High-Pressure Batch Reactions. The high-pressure reactions were carried out by pressurizing the entire ultrahigh vacuum (UHV) chamber (61.6 L) with O_2/CO gaseous mixtures and then subsequently heating the Pd and Pt samples (located within the infrared cell) at various temperatures. The reaction rate was calculated using the pressure change of the reactant mixture, as determined by a baratron manometer. PM-IRAS spectra were acquired at each reaction temperature to monitor the surface CO species. CO conversion was generally kept below 10% to obtain differential reaction rates.

Figure 4a displays a typical example of a reaction cycle using an O_2/CO (1/1) mixture at an initial CO pressure of 8 Torr. The thick solid line represents the change in pressure and the thin ladder-like line represents the reaction temperature. The number above each step shows the corresponding reaction rate (TOF) at that temperature. Figure 4b shows the corresponding PM-IRAS spectra at various reaction temperatures. As has been described in the previous paper,¹ three reaction regimes are noticed. In the first regime (reaction temperature ≤ 575 K), the surface is metallic and covered with CO at coverages higher than 0.5 ML (judged by the vibrational frequency, see explanation below). In this case, the reaction is determined predomi-

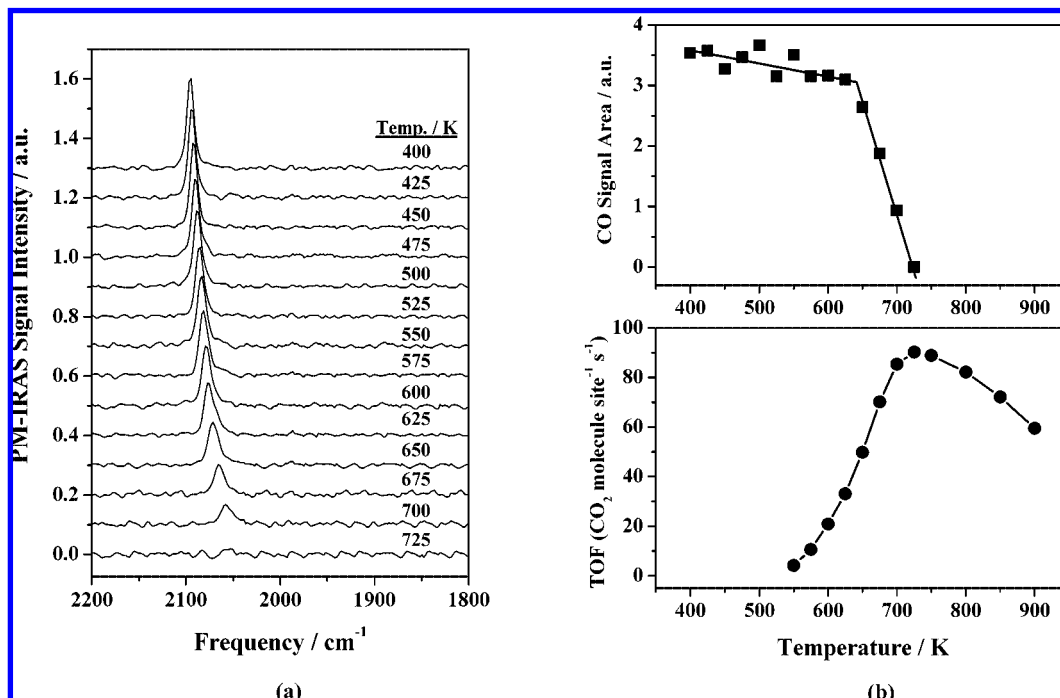


Figure 3. (a) PM-IRAS spectra of O_2/CO (1/1) mixture over Pt(110) at CO pressure of 1×10^{-3} Torr as a function of temperature. Sample temperatures are marked adjacent to each spectrum. (b) CO PM-IRAS signal area (upper panel) and CO₂ formation rate (TOF) versus reaction temperature. Note that surface CO species becomes almost undetectable when CO₂ formation rate maximizes.

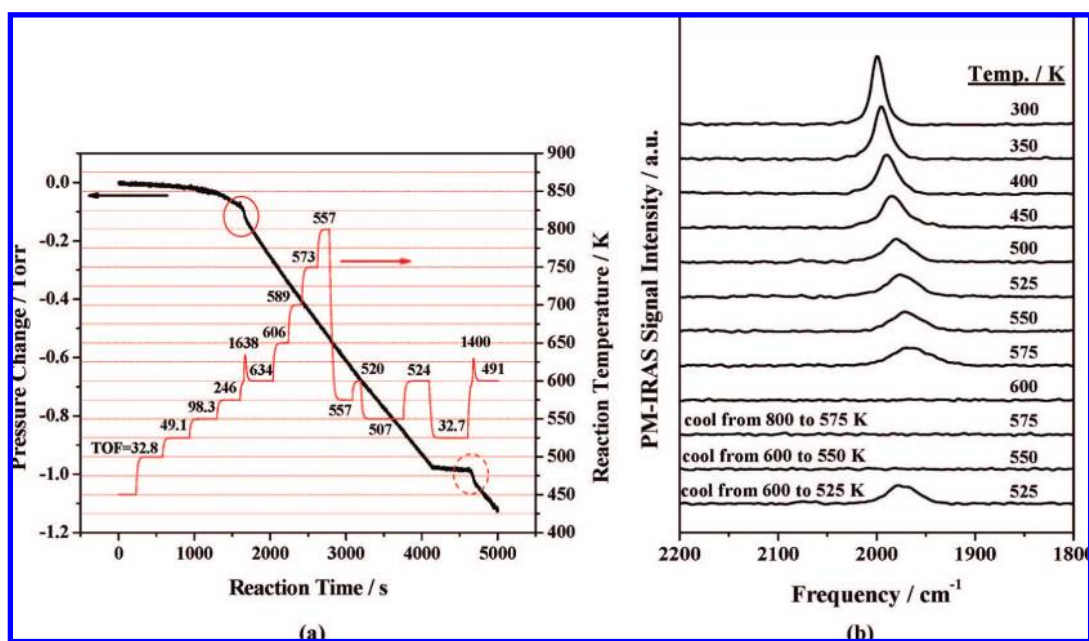


Figure 4. (a) Gas-phase pressure change (thick line) and reaction temperature (thin ladder-like line) as a function of reaction time over Pd(100). Initial reactant is an O_2/CO (1/1) mixture at CO pressure of 8 Torr. Numbers marked above each temperature are the corresponding reaction rates (TOF). Specific portions of the pressure change line are marked with solid and dashed cycles (see text for details). (b) CO PM-IRAS spectra as a function of temperature where sample temperature is marked adjacent to the corresponding spectrum. Note that bridging CO species is detected in the low-rate regime while no CO species is detectable in high-rate regimes.

nately by CO desorption, evidenced by the fact that (1) the CO₂ formation rate increases with increasing reaction temperature and (2) the reaction activation energy is approximately the same as desorption activation energy of CO.¹⁰ As the sample temperature is first increased from 575 to 600 K, the second regime appears. In this case, the reaction rate increases greatly (marked with a solid circle on the pressure curve). The highest reaction rate is a transient rate corresponding to a TOF of ~ 1600 . As a consequence, because of the exothermic nature of the reaction, the sample temperature increased ~ 30 K momen-

tarily. As will be shown below, no adsorbed CO is detected on the surface in this regime, consistent with the surface being oxygen-rich. The third regime (mass transfer limited regime from reaction time ~ 1730 to ~ 4100 s) is reached immediately after the second regime. In this case, the CO₂ formation rate becomes independent of the reaction temperature and dependent only on the rate of CO diffusion to the sample. As shown in Figure 4a, the slight TOF decrease with reaction time is due more to CO consumption rather than reaction temperature variation in this regime. To interrupt this mass transfer limited

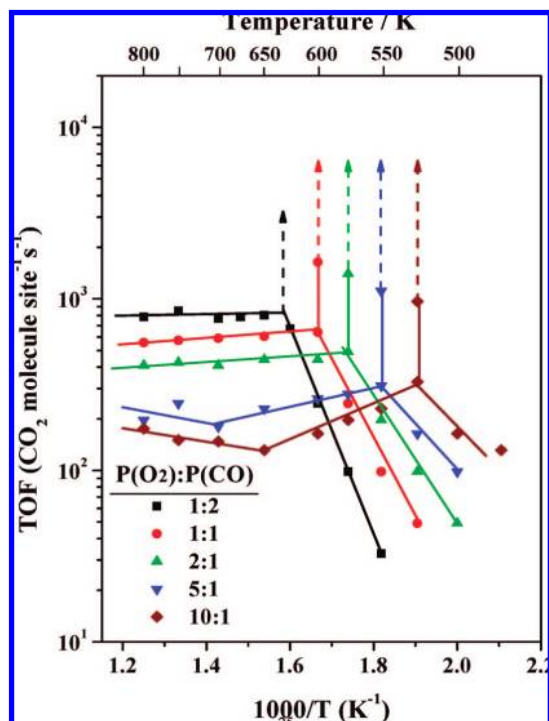


Figure 5. Arrhenius plots of CO_2 formation of 1/2 (■), 1/1 (●), 2/1 (▲), 5/1 (▼), and 10/1 (◆) O_2/CO mixtures at initial CO pressure of 8 Torr over Pd(100). Transient reaction rate jump is highlighted with arrows.

regime, the sample must be cooled to 525 K or less (reaction time from ~ 4100 to ~ 4600 s) in order to slow the reaction and to allow CO to repopulate the surface and near-surface region. Following this step, the second and the third regimes reappear when the sample is again annealed to 575 K (marked with a dashed cycle in the pressure curve). This process can be repeated as long as sufficient reactants are present.

Figure 5 displays Arrhenius plots of a series of reactions carried out over Pd(100) with reactants of various O_2/CO ratios while maintaining the CO pressure at 8 Torr; the data shown in Figure 4a are included for reference. In all cases the reaction can be divided into the three regimes described above: (i) a CO-inhibited low-temperature regime; (iii) a high-temperature regime (which may or may not be mass transfer limited, see explanation below); and (ii) a transient, high-rate regime between (i) and (iii). It is noteworthy that for very oxidizing mixtures ($\text{O}_2/\text{CO} \geq 5$), the reaction rate decreases first with increasing temperature in the third regime and, as the reaction temperature is further increased to 650–700 K, the reaction rate increases again. During these experiments, CO conversion is kept below 10% in order to keep the O_2/CO ratio relatively unchanged.

Figure 6 presents the corresponding PM-IRAS spectra acquired during the experiments shown in Figure 5 (a portion of Figure 4b is also included). In all cases, the spectra acquired prior to the roll over points show ν_{CO} with frequencies higher than $\sim 1960 \text{ cm}^{-1}$ consistent with the CO coverages being higher than $\sim 0.6 \text{ ML}$.⁸ Under such reaction conditions the CO_2 formation rate is determined entirely by CO desorption. Indeed, the activation energy for the reaction measured in this regime is very close to the CO desorption energy. Spectra acquired immediately after the roll over points, however, depend critically on the O_2/CO ratio. For reactants with initial O_2/CO ratios ≤ 2 , no CO species are detected after the roll over points. For reactants with O_2/CO ratios ≥ 5 , however, following the rate

roll over, CO species appear with vibrational frequencies at 2142 and 2087 cm^{-1} . For 10/1 mixtures, the 2142 cm^{-1} feature blue shifts slightly at 550 and 575 K. It is noteworthy that the appearance of these new CO species shows that the nature of the Pd surface has changed. Moreover, the CO_2 formation rate decreases to a value below the mass transfer limiting rate in the temperature range where these two CO species coexist on the surface (Figure 5). Identical experiments were also performed over Pd(111) and Pd(110) surfaces, and the results obtained were essentially identical; in particular, the 2142 and 2087 cm^{-1} features also form at high O_2/CO ratios, demonstrating that a common surface is involved.

During the high-pressure experiments described above, it was difficult to spectroscopically monitor the CO surface species within the second regime, i.e., the transient regime with high reaction rates, primarily because this regime only lasts for less than 1 min. In order to monitor the rather short duration of this regime, continuous infrared scans were carried out near the roll over point with each spectrum acquired by superimposing only five scans (total collection time ~ 5.3 s). This is the shortest acquisition time that can provide a spectrum with reasonable quality. As shown in Figure 7, when the Pd(100) sample is exposed to an O_2/CO (10/1) mixture at 500 K (CO initial pressure 2 Torr), the surface maintains its metallic character within the first ~ 120 s; i.e., the surface is covered by CO with a vibrational frequency at $\sim 1980 \text{ cm}^{-1}$. The calculated TOF in this regime is 110 ± 30 . Subsequently the reaction rate increases rather abruptly and sustains this high rate for ~ 40 s during which a TOF of 1150 ± 350 is reached. Interestingly, there is no detectable CO species on the surface within this regime. Finally the third regime is apparent where the surface is covered with CO species at 2140 and 2087 cm^{-1} . In this case, a TOF of 250 ± 70 is measured. These results, together with data acquired at low and high pressures at all O_2/CO ratios, demonstrate that at the point of the highest reaction rate for any given O_2/CO ratio and pressure, the surface CO coverage is virtually zero.

It is evident that the second regime described above occurs rapidly and is transient in nature because of mass transfer effects. As such, efforts were made to extend the experimental time scale of this regime to enable further study. One approach is to carry out the CO oxidation reaction with the sample in the center of the main (larger volume) chamber rather than in the infrared cell. As will be shown below, heat generated during the reaction promotes reactant circulation using this approach. Alternatively, the gases can be circulated using a pump. Figure 8 displays an example of a reaction over Pd(100) with a stoichiometric O_2/CO (1/2) mixture at a CO initial pressure of 8 Torr. In this experiment, the sample is placed in the center of the main chamber. The bottom panel plots gas pressure and the upper panel plots the reaction temperature, both as a function of reaction time. Some reaction rate (TOF) values are also marked adjacent to the corresponding temperatures in the upper panel. In this case, the surface is dominated with CO below 625 K and the reaction kinetics appears to be identical to those obtained in the infrared cell. When trying to anneal the sample from 625 to 650 K, a “light off” phenomenon occurs such that the reaction rate increases dramatically as indicated by the sharp gas-phase pressure drop and the increase of the sample temperature to as high as 1150 K. The reaction becomes self-sustaining thereafter until the majority of the reactants are consumed. This experiment demonstrates that reaction heat induces reactant circulation, thus partially breaking down the mass transport constraints. This conclusion can be drawn straightforwardly by comparing reaction rates shown in Figures 5 and 8 at the same sample

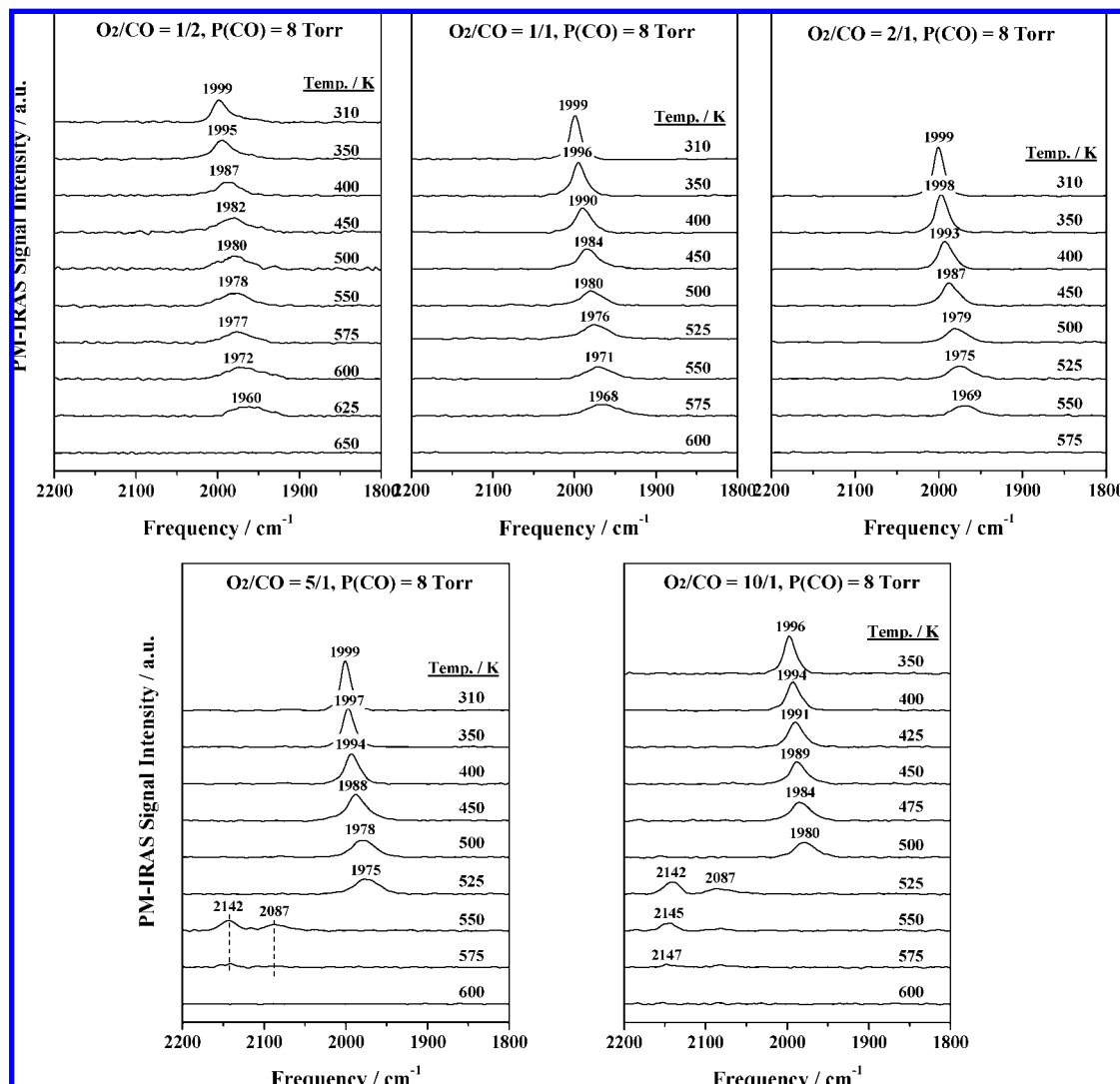


Figure 6. PM-IRAS spectra as a function of reaction temperature over various O_2/CO mixtures at initial CO pressure of 8 Torr over Pd(100). O_2/CO ratios are displayed within the top part of each panel, and sample temperatures are marked adjacent to each spectrum.

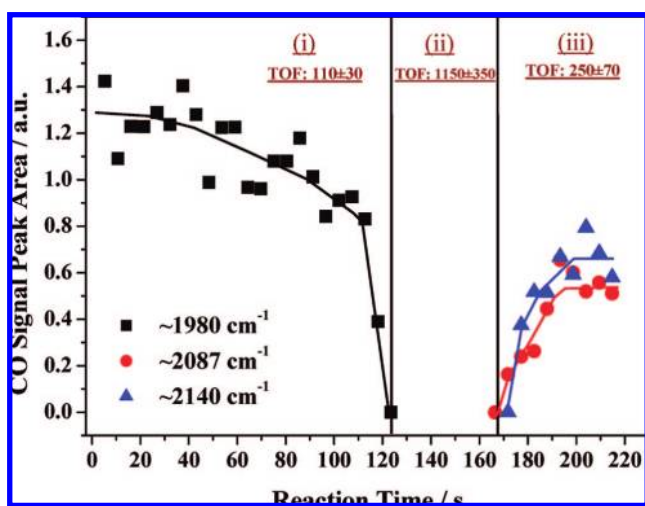


Figure 7. Areas of CO PM-IRAS signals at 1980 (■), 2087 (●), and 2140 (▲) cm^{-1} as a function of reaction time. Initial reactant is an O_2/CO (10/1) mixture at a CO pressure of 2 Torr, and reaction is carried out at 500 K. Reaction is divided into three regimes (see text), and reaction rate (TOF) in each regime is displayed.

temperatures. As displayed in Figure 5, at a sample temperature of 700 K, a TOF is measured well below 1000 when the Pd(100)

sample is placed inside the infrared cell at any O_2/CO ratio. However Figure 8 shows a TOF of ~ 1600 at the same temperature when the sample is placed inside the main chamber. This phenomenon has been found by Su et al. over Pt(111) under similar reaction conditions.¹¹ We have also shown previously that by using samples with reduced sizes, mass transport constraints can also be partially circumvented thus facilitating higher reaction rates.⁷

Similar high-pressure experiments were also carried out on Pt(110). Figure 9 displays Arrhenius plots of reactions carried out with gas reactants of various O_2/CO ratios with an initial CO pressure of 8 Torr. Again, CO conversion remains below 10% during these experiments. As seen previously, three reaction regimes are evident. However for Pt(110), there is no apparent variation of the CO_2 formation rate within the mass transfer limited regime. Figure 10 plots the corresponding PM-IRAS spectra. Clearly the surfaces are CO-covered within the low-temperature regime while no CO species are found within the second and third regimes. In other words, the PM-IRAS data provide no evidence for the oxidation of Pt; i.e., no CO species associated with Pt oxides are detected. Finally experiments were carried out using reactants with an O_2/CO ratio equal to $\sim 35/1$ and an O_2 pressure of ~ 0.5 bar, conditions very similar to those used by Frenken et al.⁴ At a reaction temperature of

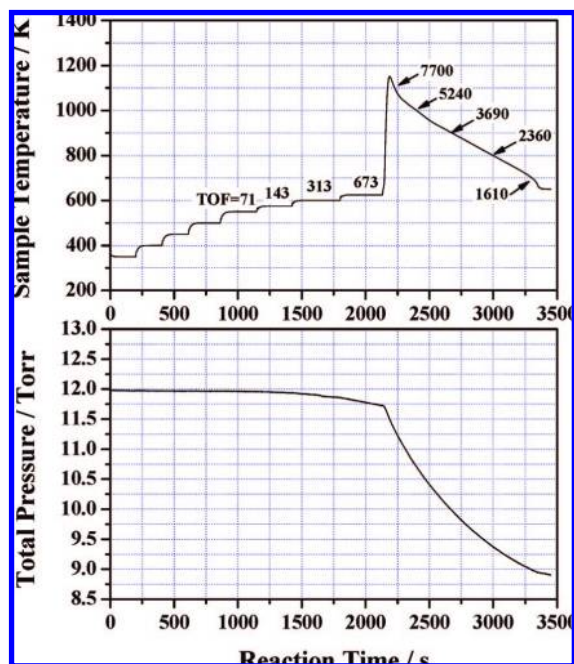


Figure 8. Gas-phase pressure (bottom panel) and sample temperature (upper panel) vs reaction time for an O_2/CO (1/2) mixture at an initial total pressure of 12 Torr. Experiment is performed with the Pd(100) sample staying in the center of the main chamber. At selected sample temperatures, corresponding reaction rate (TOF) values are marked.

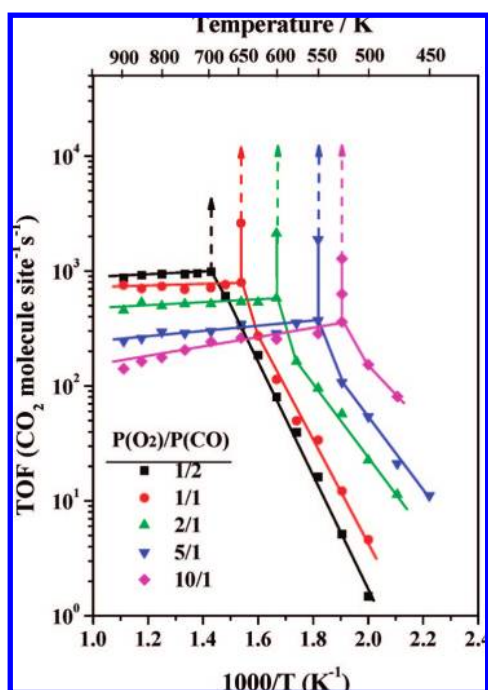


Figure 9. Arrhenius plots of CO_2 formation of 1/2 (■), 1/1 (●), 2/1 (▲), 5/1 (▼), and 10/1 (◆) O_2/CO mixtures at initial CO pressure of 8 Torr over Pt(110). Transient reaction rate jump is highlighted with arrows.

425 K, the temperature at which the authors claimed to discover the “superior oxide reactivity”, our results show that the Pt(110) sample is fully covered by CO and the reaction rate is barely measurable. This reaction condition could be maintained for hours of operation. Only when the sample is carefully heated to 480 K do the second and third reaction regimes appear (Figure 11). Because the CO component is so dilute in the reactant mixture, only ~ 1 K increase of the sample temperature during

the second regime is evident, and the reaction rate is only slightly higher than the third regime, i.e., the mass transfer limited regime. Moreover, during the second and third regimes, no surface CO species is detectable; i.e., there is no PM-IRAS evidence for oxidation of Pt under these conditions.

4. Discussion

We begin the discussion by summarizing a few key observations from the steady-state reaction results performed on Pd and Pt surfaces at low pressures ($P_{\text{CO}} \leq 1 \times 10^{-3}$ Torr). First, CO inhibition but no O inhibition is observed under any reaction conditions including very high O_2/CO ratios. Second, CO conversion is collision limited at low pressures. This is evident in that CO conversion when optimized is inevitably near 40% at CO pressures below $\sim 1 \times 10^{-4}$ Torr (Figure 2). Moreover, the optimized CO conversion is independent of the O_2/CO ratio at any CO pressure $\leq 1 \times 10^{-4}$ Torr. This behavior implies common CO and O coverages at the optimized reaction conditions, even though the gas phase compositions and reaction temperatures are varying. Third, under optimized reaction conditions, the surface CO coverage is always extremely low, i.e., below the detection limit of IRAS. In contrast, the surface oxygen coverage is much higher. Although we do not know the precise optimized oxygen coverages, previous studies using X-ray photoelectron spectroscopy (XPS) indicated an oxygen coverage of ~ 0.5 ML on Pd(110);¹² a rather wide range of oxygen coverages between 0.3 and 0.7 ML for the (1×2) reconstructed Pt(110) was measured with photoelectron emission microscopy (PEEM).¹³ These results suggest that removal of the CO inhibition is more critical to CO_2 formation than is the oxygen coverage.

Before discussing the high-pressure results, we would like to emphasize again the importance of mass transfer in limiting the reaction rate, a consideration frequently overlooked in previous studies.¹⁴ Mass transfer begins to limit the reaction rate at that point where the reaction rate exceeds the rate at which the limiting reactant can diffuse to the catalyst surface. Since the mean free path of gas molecules decreases with an increase in pressure, this effect can become important at pressures as low as $\sim 1 \times 10^{-3}$ Torr. As shown in Figure 2, a decrease in the CO conversion is evident as the CO pressure reaches 1×10^{-3} Torr; similar results were found for Rh(111).¹ As a consequence, under reaction conditions with no mass transfer constraints, the optimized CO conversion reaches $\sim 40\%$ of the incident CO flux. However, at a CO pressure of 8 Torr, the CO conversion is only $\sim 0.34\%$ of the incident CO flux at the highest CO conversion conditions (TOF ~ 8000 , Figure 8). The limits of mass transfer of CO in high pressures of oxygen-rich reactants lead to significant enrichment of O_2 near the sample to such an extent that the O_2/CO ratio near the sample can be orders of magnitude higher than the O_2/CO ratio in the overall reactants. Given that the oxidized sample is less reactive, limits in mass transfer can lead to reaction oscillation as is frequently observed.¹⁵

Under stoichiometric and mildly oxidizing reaction conditions ($\text{O}_2/\text{CO} \leq 2$), high-pressure kinetic data for Rh,¹ Pd (Figure 5), and Pt (Figure 9) are very similar. Differences in reaction rate (TOF) arise mainly because the rate is calculated on a per surface site basis. If the reaction rate is calculated on a per surface area basis, the reaction rates on various metal surfaces are almost identical. This observation, often referred to as “structure insensitivity”,¹⁰ arises from the fact that in the CO-inhibited regime, the reaction is largely controlled by CO desorption. Since the CO binding energy on various Pt-group

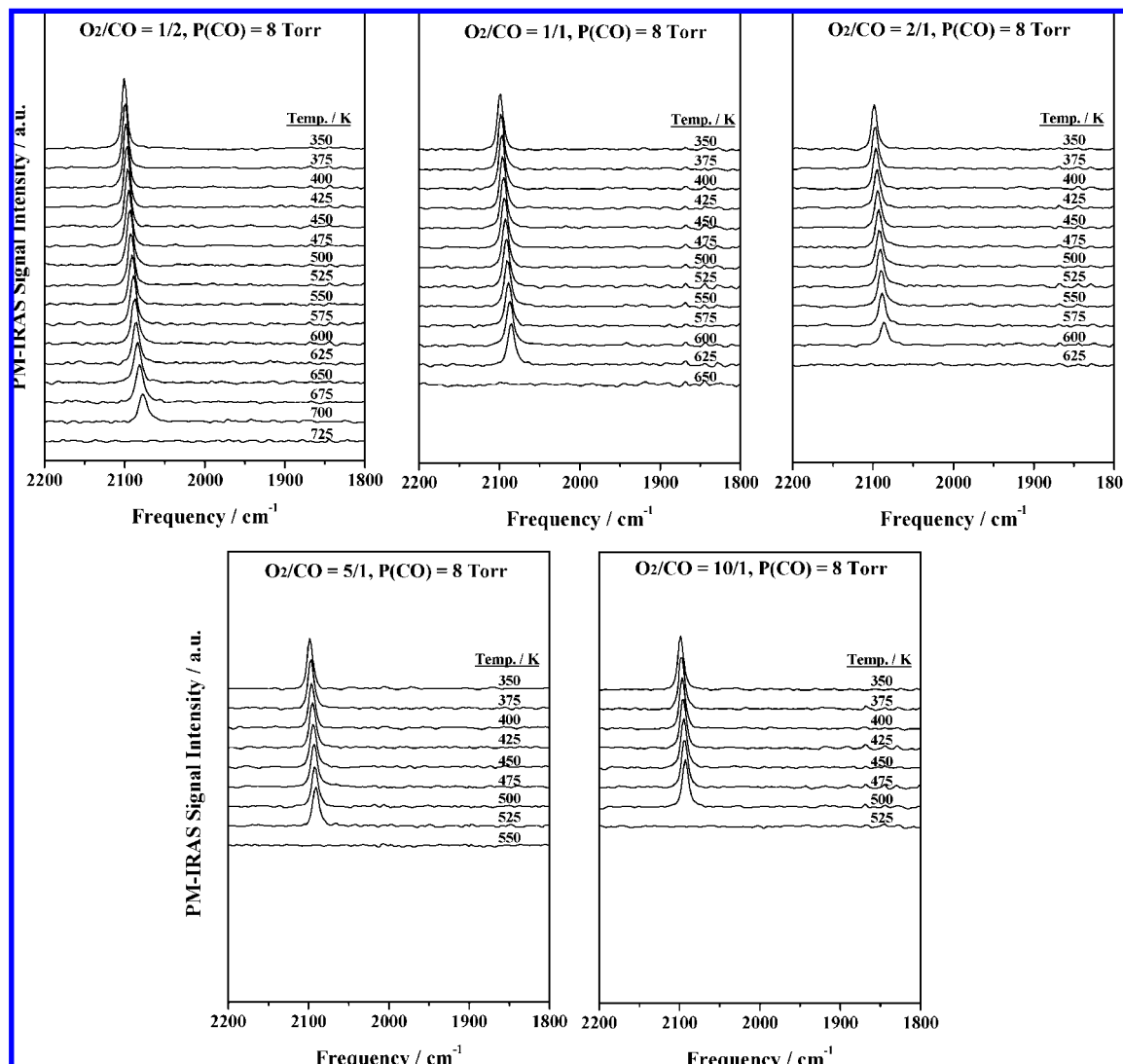


Figure 10. PM-IRAS spectra as a function of reaction temperature over various O_2/CO mixtures at initial CO pressure of 8 Torr over Pt(110). O_2/CO ratios are displayed within the top part of each panel, and sample temperatures are marked adjacent of each spectrum.

metals is very similar;⁸ it follows that the corresponding reaction rates should also be similar. Within the mass transfer limited regime, the reaction kinetics must be identical for various catalysts, as found experimentally. Although a degree of structure sensitivity can be envisioned within the second regime, no detailed analysis at present is possible for this transient reaction region.

Under heavily oxidizing reaction conditions ($\text{O}_2/\text{CO} \geq 5$) and at high temperatures, the behavior of the various noble metals becomes very different. For Pt(110), as shown in Figure 9, the CO_2 formation rate remains constant within the third regime (the slight drop in the rate at very high temperatures is due mainly to the high CO conversion) demonstrating that the reaction is controlled by mass transfer and the reactivity of the surface remains constant within the entire regime. As displayed in Figure 10, no CO surface species is detectable within the second and third regimes. These results are consistent with but do not prove that the metal surface is reduced. However, the results for Pd provide clear evidence of Pd oxidation by the emergence of new CO species at 2142 and 2087 cm^{-1} ; these species are not present on the metallic Pd(100) surface. The precise nature of this oxidized phase, i.e., its composition, thickness, etc., is not known at present; however, we can reach some tentative conclusions. First of all, this oxide phase is not

likely to be bulk PdO. As has been shown previously, in order to form bulklike PdO on a Pd(100) surface, oxygen partial pressures beyond 1 mbar and sample temperatures exceeding 650 K are required. In fact, ~ 1200 s is required for the transformation from the $(\sqrt{5} \times \sqrt{5})\text{R}27^\circ$ surface oxide to PdO bulk oxide at 675 K and 50 mbar O_2 pressure.¹⁶ Second, this oxide phase is unlikely to be a specific (two-dimensional (2D)) surface oxide, e.g., the $(\sqrt{5} \times \sqrt{5})\text{R}27^\circ$ surface oxide. This argument follows since identical PM-IRAS spectra are obtained in the third regime on Pd(110), -(100), and -(111) surfaces, i.e., all spectra display 2142 and 2087 cm^{-1} features with almost identical relative intensities at identical reaction conditions (temperature, gas pressure, and gas phase composition). These findings indicate that a common oxidized phase is formed. Therefore we conclude, tentatively, that a 3D surface oxide phase forms at the onset of the third regime. More interestingly, within the temperature range (525–650 K) where this surface oxide exists, the CO_2 formation rate apparently decreases with increasing temperature. In other words, the reaction rate falls below the mass transfer limiting value. This behavior can only be explained by deactivation of the metal surface.¹ More convincing evidence regarding the relative low reactivity of the oxide phase is the fact that the CO_2 formation rate begins to increase again from 650 to 800 K. This increase in reactivity is

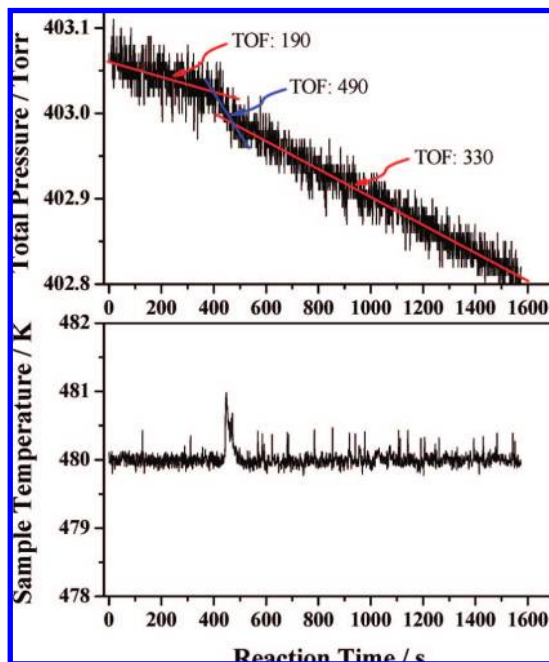


Figure 11. Gas pressure (upper panel) and sample temperature (bottom panel) vs reaction time over Pt(110). Initial O_2/CO ratio is $\sim 35/1$ and total pressure is ~ 403 Torr. Note that there are three distinct regimes (see text) and reaction rate (TOF) in each regime is displayed.

very likely related to the fact that the Pd surface oxide begins to dissociate precisely within this temperature threshold.¹⁷ Additional evidence supporting the superior reactivity of the reduced metal surface are the data shown in Figure 8. By circumventing to some extent the mass transfer constraints, the CO_2 formation rate can reach a TOF ~ 7700 at 1150 K. Clearly no Pd oxide is stable at this temperature, therefore the sample must be metallic. Note also that at such a high temperature the resident time for CO and O on the surface is extremely small; however, even under this nonoptimized reaction condition on a metallic surface, the CO_2 formation rate is much higher than that on an oxide surface. Overall, the combination of data shown in Figures 5, 6, and 8 allows us to conclude that the reactivity of Pd surfaces decreases upon oxidation. For Pt(110), under reaction conditions where Pd oxidizes, reaction kinetics (Figure 9) and PM-IRAS (Figure 10) suggest that oxidation of the surface has not occurred.

Finally, we would like to comment on the incorrect conclusions of Frenken et al.^{4–6} Under reaction conditions and sampling capabilities such as those used by Frenken et al.^{4–6} i.e., very high O_2/CO ratio conditions and a rather long time constant for product analysis, one can easily jump from regime (i) to regime (iii) without detecting regime (ii). We believe Frenken et al. failed to observe the second critical reaction regime during their studies. With Pd(100) as an example (Figure 7), in the first regime the Pd surface is CO inhibited and the CO_2 formation rate is low (TOF $\sim 110 \pm 30$); in the third regime the Pd surface is oxidized, however the CO oxidation rate is comparable (TOF $\sim 250 \pm 70$). Solely on the basis of this coincidence of rates for the CO-inhibited surface and the oxidized surface, the authors claim that an oxide phase has a higher reactivity than the metal phase. Obviously such a claim is in error since comparing reactivity of any particular surface with a CO-inhibited metal surface is dubious given the reactivity of the CO-inhibited surface is exceedingly low for the reasons discussed above. Under the same reaction conditions, a CO-uninhibited metal surface displays much higher reactivity (TOF

$\sim 1150 \pm 350$) despite being mass transfer limited. For Pt(110), however, as shown in Figure 11, by omitting the second regime and assuming that the surface is oxidized in the third regime, one can draw the incorrect conclusion as does Frenken et al.⁴ that the oxide surface is more reactive. However, during the course of this study, we found no evidence (based on reaction kinetics and PM-IRAS) for oxidation of Pt(110). The conclusion drawn by Frenken et al.⁴ for the Pt(110) system that roughing of the Pt(110) surface corresponded to oxidation of the surface is very likely incorrect. It is noteworthy that recently, using surface X-ray diffraction, Frenken et al. reported the formation of Pt surface oxides at 625 K,¹⁸ a temperature far beyond that used in their initial report, 425 K.⁴ Finally, a recent study regarding Pt(110) oxidation revealed that in order to form a stable surface oxide, the chemisorption phase and the surface oxide phase must coexist (their ΔG values must cross) at a $\Delta\mu_0$ for which the bulk oxide has not yet formed.¹⁹

5. Conclusions

We have shown that CO oxidation on Pd and Pt surfaces displays no discontinuities between low and high pressures; i.e., there is no pressure gap. The chemisorbed oxygen-dominated surface, responsible for the high CO_2 formation rate at low pressures, is also the most active phase at high pressures. However, due to the complexity of high-pressure reactions, especially the limitations of mass transfer, the high reaction rate state often is transient. Especially for reactants with very high O_2/CO ratios, this state can be easily overlooked and erroneous conclusions can be drawn, a case in point being the purported superior reactivity of oxide surfaces.^{4–6}

Acknowledgment. We gratefully acknowledge the support for this work by the Department of Energy (DOE), Office of Basic Energy Sciences, Division of Chemical Sciences under Grant Number DE-FG02-95ER14511 and the Robert A. Welch Foundation.

References and Notes

- (1) Gao, F.; Cai, Y.; Gath, K. K.; Wang, Y.; Chen, M. S.; Guo, Q. L.; Goodman, D. W. *J. Phys. Chem. C* **2009**, *113*, 182–192.
- (2) Goodman, D. W.; Peden, C. H. F. *J. Phys. Chem.* **1986**, *90*, 4839.
- (3) Kiss, J. T.; Gonzalez, R. D. *Ind. Eng. Chem. Prod. Res. Dev.* **1985**, *24*, 216.
- (4) Hendriksen, B. L. M.; Frenken, J. W. M. *Phys. Rev. Lett.* **2002**, *89*, 046101.
- (5) Hendriksen, B. L. M.; Bobaru, S. C.; Frenken, J. W. M. *Surf. Sci.* **2004**, *552*, 229.
- (6) Hendriksen, B. L. M.; Bobaru, S. C.; Frenken, J. W. M. *Top. Catal.* **2005**, *36*, 43.
- (7) Chen, M. S.; Cai, Y.; Yan, Z.; Gath, K. K.; Axnanda, S.; Goodman, D. W. *Surf. Sci.* **2007**, *601*, 5326.
- (8) Engel, T.; Ertl, G. *Adv. Catal.* **1979**, *28*, 1.
- (9) Szanyi, J.; Kuhn, W. K.; Goodman, D. W. *J. Vac. Sci. Technol., A* **1993**, *11*, 1969.
- (10) Goodman, D. W. *Chem. Rev.* **1995**, *95*, 523.
- (11) Su, X.; Cremer, P. S.; Shen, Y. R.; Somorjai, G. A. *J. Am. Chem. Soc.* **1997**, *119*, 3994.
- (12) Jones, I. Z.; Bennetta, R. A.; Bowker, M. *Surf. Sci.* **1999**, *439*, 235.
- (13) Miners, J. H.; Cerasari, S.; Efstathiou, V.; Kim, M.; Woodruff, D. P. *J. Chem. Phys.* **2002**, *117*, 885.
- (14) Fuchs, S.; Hahn, T. *Stud. Surf. Sci. Catal.* **1995**, *96*, 275.
- (15) Turner, J. E.; Sales, B. C.; Maple, M. B. *Surf. Sci.* **1981**, *103*, 54.
- (16) Stierle, A.; Kasper, N.; Dosch, H.; Lundgren, E.; Gustafson, J.; Mikkelsen, A.; Andersen, J. N. *J. Chem. Phys.* **2005**, *122*, 44706.
- (17) Kan, H. H.; Shumbera, R. B.; Weaver, J. F. *Surf. Sci.* **2008**, *602*, 1337.
- (18) Ackermann, M. D.; Pedersen, T. M.; Hendriksen, B. L. M.; Robach, O.; Bobaru, S. C.; Popa, I.; Quiros, C.; Kim, H.; Hammer, B.; Ferrer, S.; Frenken, J. W. M. *Phys. Rev. Lett.* **2005**, *95*, 255505.
- (19) Li, W. X.; Österlund, L.; Vestergaard, E. K.; Vang, R. T.; Matthiesen, J.; Pedersen, T. M.; Lægsgaard, E.; Hammer, B.; Besenbacher, F. *Phys. Rev. Lett.* **2004**, *93*, 146104.